ELSEVIER

Polymer 41 (2000) 5269–5282

polymer

Solid-state NMR study of structure, size and dynamics of domains in hybrid siloxane networks

J. Brus*, J. Dybal

Institute of Macromolecular Chemistry, Academy of Sciences of the Czech Republic, Heyrovský Sq. 2, 162 06 Prague 6, Czech Republic

Received 4 June 1999; received in revised form 10 September 1999; accepted 27 September 1999

Abstract

Structure, size and dynamics of domains of hybrid siloxane networks prepared by copolymerization of tetraethoxysilane (TEOS) and dimethyl(diethoxy)silane (DMDEOS) were studied by several techniques of solid-state ^{1}H and ^{29}Si NMR spectroscopy as well as by ab initio quantum chemical calculations. $T_{1\rho}(^{1}H)$ relaxation times, dipolar dephasing and spin diffusion experiments confirmed the existence of nano-heterogeneous system with random, bicontinuous morphology. The size of domains of TEOS homopolymer is about 1.3–2.8 nm, the size of copolymer phase being larger, ca. 4.0–6.8 nm. Quantum chemical ab initio calculations of geometry and the principal values of ^{29}Si NMR chemical shift tensor and the isotropic chemical shift confirmed our structural predictions that copolymers with polycyclic structure units are formed. The accord of calculated values with those experimentally determined was sufficiently good.

Keywords: Hybrid siloxane networks; Solid state NMR; Spin diffusion

1. Introduction

The optimum use of siloxane materials in catalysis, microelectronics, separation, photon based technologies, etc. requires perfect knowledge of their structure. ^{1}H, ^{13}C, and ^{29}Si NMR spectroscopy [1–8] as well as quantum chemical calculations [9] have been utilized to investigate kinetics and mechanisms of initial stages of formation of these materials. In the studies of the structure of the resulting products; a variety of solid-state NMR techniques (^{1}H MAS [10], ^{1}H CRAMPS [11], ^{29}Si CP/MAS [10,12–21]) have been used. They brought a basic information about the nature and properties of adsorbed water and the structure of the siloxane network. So far, the best-explored material has been a product prepared by polycondensation of tetraethoxysilane (TEOS). Recently, modified hybrid inorganic–organic materials, which have more acceptable properties [22–25], have appeared in the field of general interest. However, structure and dynamic properties of these modified siloxane networks have not been sufficiently described yet, although they determine final properties of these materials.

In our previous work [26] we studied the initial stages of copolymerization of TEOS and dimethyl(diethoxy)silane (DMDEOS). It was proved that differences in reactivity of both monomers cause formation of a diverse mixture of reaction products containing copolymers as well as homopolymers of both types of monomers. The arising copolymer contains a higher amount of DMDEOS monomer units (ca. 70 mol%). Hence the final product is probably a partially heterogeneous or nano-heterogeneous system containing regions of statistic copolymer and domains of TEOS units.

In this paper, we evaluated the effect of copolymerization of DMDEOS with TEOS on the structure and dynamic behavior of the resulting siloxane networks. We tried to characterize the structure of siloxane networks prepared by copolymerization of TEOS and DMDEOS and to compare them with the structure of homopolymer network composed only from TEOS units. The behavior and properties of silanol groups and adsorbed water, and overall geometry and structure of siloxane network using ab initio and molecular mechanics calculations were evaluated. For these purposes, several advanced solid state NMR techniques were used.

2. Experimental

2.1. Preparation of siloxane materials

Glassy siloxane materials, sometimes called gels, were

* Corresponding author. Tel.: +420-2-2040-3380; fax: +420-2-367-981.
E-mail address: brus@imc.cas.cz (J. Brus).

0032-3861/00/$ - see front matter
PII: S0032-3861(99)00741-7

Table 1
Composition of reaction mixtures

No.	Molar ratio	Code
1	TEOS[a] /C_2H_5OH[c] /H_2O/HCl 1/4.50/1/0.03	**TE**
2	TEOS/DMDEOS[b] /C_2H_5OH/H_2O/HCl 0.5/0.5/4.50/1/0.03	**TE-DM-1-1**
3	TEOS/DMDEOS/C_2H_5OH/H_2O/HCl 0.75/0.25/4.50/1/0.03	**TE-DM-3-1**

[a] TEOS—Synthesia Kolín, Czech Republic.
[b] DMDEOS—Wacker-Chemie GmbH., Germany.
[c] Ethanol, 0.1% (w/w) water—Merck, Germany.

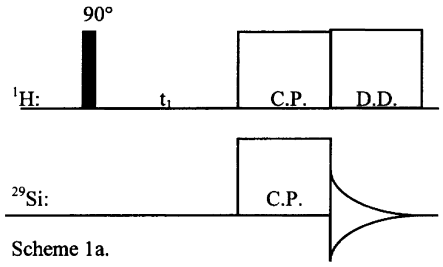

Scheme 1a.

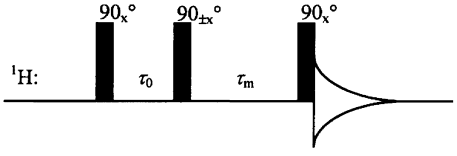

Scheme 1b.

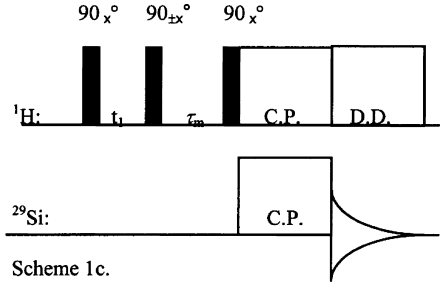

Scheme 1c.

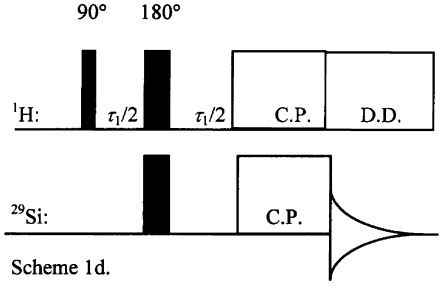

Scheme 1d.

Scheme 1.

prepared by acid-catalyzed sol–gel polycondensation of the reaction mixture, whose composition is listed in Table 1. Polymerization took place in Petri dishes under laboratory conditions. After two months from the starting of polymerization, the products were placed into an air-conditioned box (relative humidity—RH = 55%, $t = 25$°C) for 21 days at least.

2.2. NMR spectroscopy

NMR spectra were measured by using Bruker DSX 200 NMR spectrometer in 4 mm ZrO_2 rotor at frequencies 39.75 and 200.14 MHz (^{29}Si and ^{1}H, respectively). The number of data points was 6 K, magic angle spinning (MAS) frequency 0–18 kHz, strength of B_1 field (^{1}H and ^{29}Si) 62.5 kHz. The number of scans for accumulation of ^{29}Si CP/MAS NMR spectra [27] was 3600, repetition delay 10 s and spin-lock pulse 2–5 ms. Single-pulse experiments were measured with 45°-pulse length and 600 s repetition delay. The number of scans was 320. ^{29}Si scale was calibrated by the external standard M_8Q_8 (−109.8 ppm; the highest field signal). In measurements of ^{1}H MAS NMR spectra the number of scans was 32–256 and repetition delay 10 s. The external standard HMDS (hexamethyldisiloxane) was used for calibration of the ^{1}H scale, the ^{1}H chemical shift of having the value of 0.05 ppm referred to as TMS (tetramethylsilane).

T_1(^{1}H) relaxation time was determined by using the standard pulse sequence "inversion recovery" at temperatures 303, 318, 333 and 345 K and MAS at 7 kHz. Variable and relaxation delays were 0.01–20 and 20 s, respectively. The number of scans was 8.

$T_{1\rho}$(^{1}H) relaxation time was determined by using standard pulse sequence with direct detection of proton magnetization at temperatures 303, 318, 333 and 345 K with MAS at 7 kHz. Variable spin lock pulse and relaxation delay were 0.0001–0.05 and 20 s, respectively. The number of scans was 16.

Two-dimensional (2D) WISE spectroscopy [28,29] employed ^{1}H 90° pulse of 4.0 μs and 160 scans per increment. The proton evolution period (t_1) between ^{1}H 90° pulse and contact pulse consisted of 512 increments of 5 μs (cf. Scheme 1a). Total t_1 FID resolution is then 400 Hz, which was sufficient to observe relatively narrow proton signals. CP contact pulse was set relatively short (1 ms) to restrict the spin diffusion to a minimum, the rate of sample rotation was 5 kHz and the repetition delay 2 s. Signal-to-noise ratio was still sufficiently high.

1D (one-dimensional) and 2D spin-diffusion experiments were used to yield information about intermolecular distance by means of spin diffusion:

1. The Goldman–Shen pulse sequence [30] (cf. Scheme 1b) was used to study the spin diffusion on the basis of the differences in T_2. Delay τ_0 as "T_2 magnetization filter" was set equal to 200 μs so that magnetization of strongly dipolar coupled protons was completely dephased.

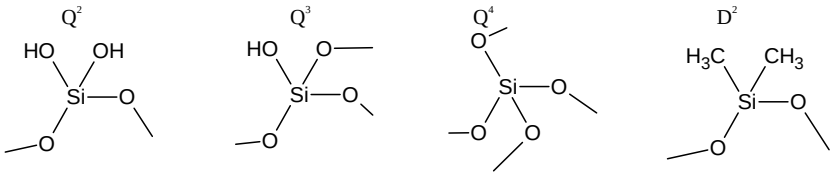

Scheme 2.

Although the T_1 relaxation limits the maximum domain size that can be determined by the proton spin diffusion experiment, for samples with a spatially constant relaxation time, its effect can be simply eliminated by an appropriate phase cycle of the pulses before the mixing time. Selected proton magnetization is aligned along $-z$ and $+z$ axes in alternating scans. All signal contributions caused by T_1 relaxation are cancelled. This increases the range of mixing times that can be exploited up to T_1. The variable mixing time τ_m was changed from 100 μs to 750 ms.

2. 2D WISE pulse sequence [28,31,32] with evolution time t_1 and spin diffusion mixing time τ_m was used to study the spin diffusion of heteronuclear dipolar coupled protons.

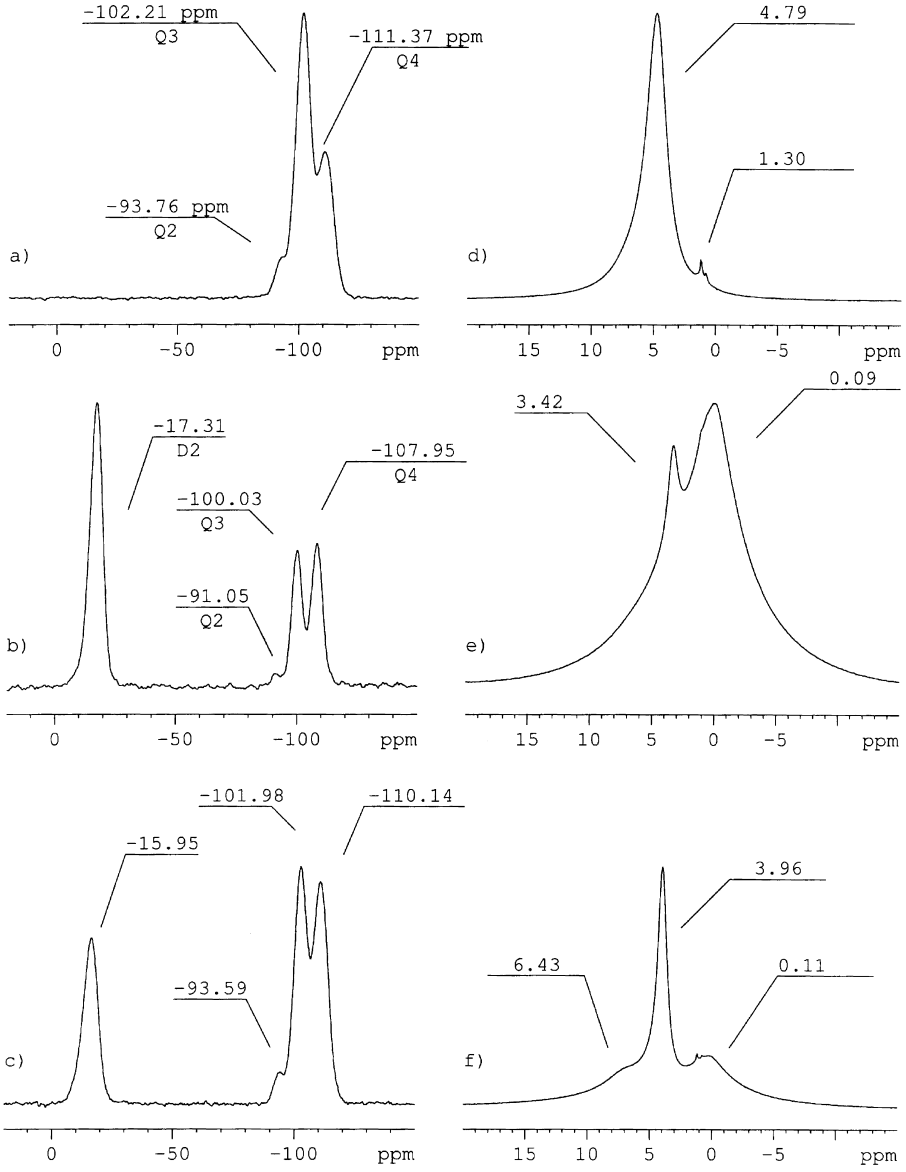

Fig. 1. ^{29}Si CP/MAS NMR (left) and ^{1}H MAS NMR (right) spectra of the products: **TE**—(a) and (d); **TE-DM-1-1**—(b) and (e); **TE-DM-3-1**—(c) and (f).

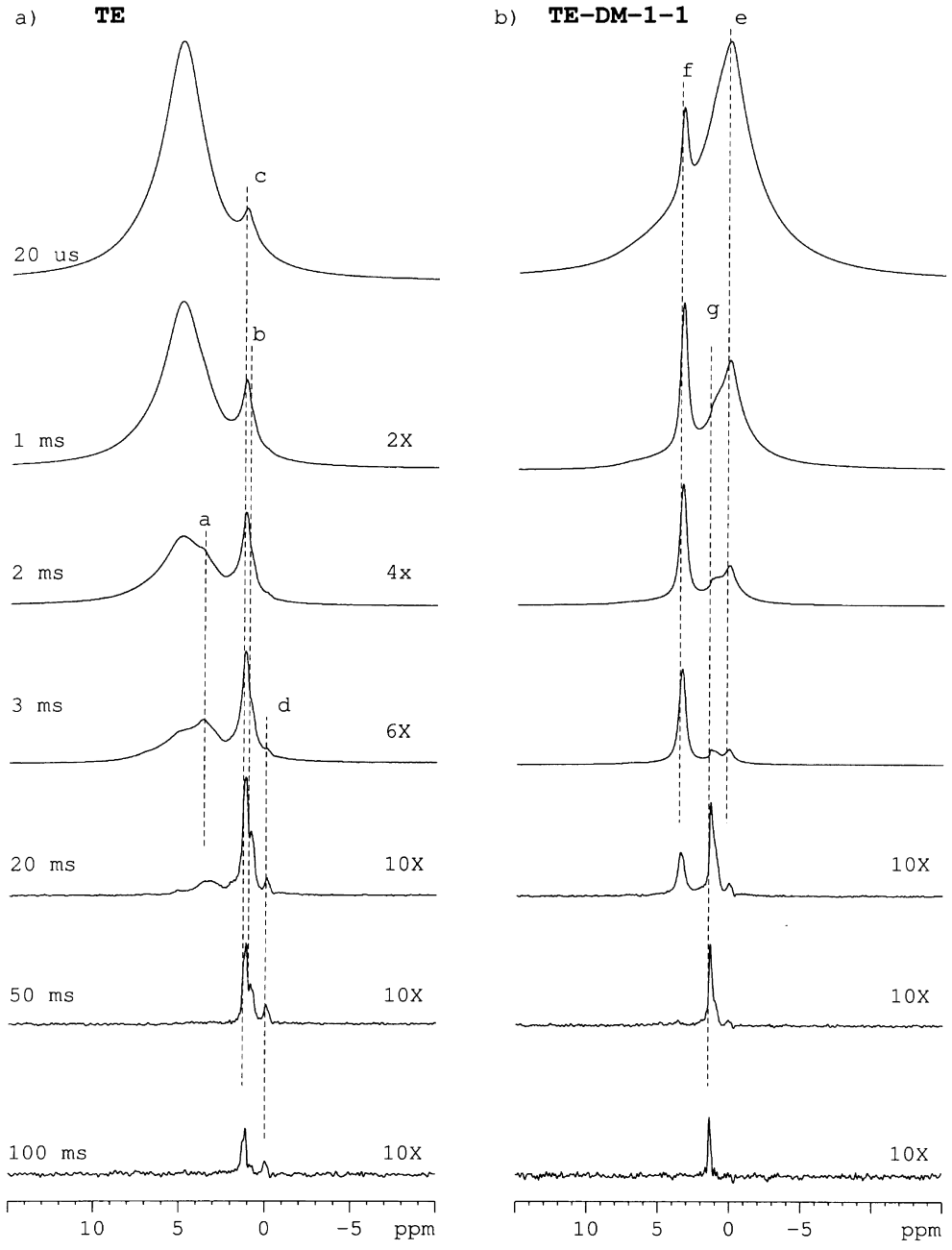

Fig. 2. ^{1}H MAS NMR spectra measured with the Hahn-echo pulse sequence ($\pi/2-\tau-\pi-\tau-$aq) of products **TE** and **TE-DM-1-1** in the columns (a) and (b), respectively. The dephasing time 2τ is aligned on the left-hand side. Number of scans increases with increasing dephasing time from 32 to 1024. For dipolar dephasing time larger than 3 ms, the spectral width is reduced from 150 kHz to 20 kHz, the number of data points is increased to 32 K to resolve the very narrow line (FID resolution was then 0.6 Hz per point). MAS frequency was 18 kHz.

Mixing time was set to 20 ms; other parameters were the same as in standard WISE experiments described above (cf. Scheme 1c).

^{1}H–^{1}H dipolar dephasing of heteronuclear dipolar-coupled protons was studied by using standard pulse sequence [21,33] with two 180° refocusing pulses in both channels (^{1}H, ^{29}Si) to remove phase distortion (cf. Scheme 1d). MAS frequency was 5 kHz, dipolar dephasing time was in the range of 0–1 ms, number of experiments 256, number of FID accumulations per one experiment 160, and repetition delay 2 s.

2.3. Geometry optimization

Ab initio calculation and molecular mechanics calculation: The calculations were run on SGI workstations using GAUSSIAN 94 and INSIGHT II program packages [34,35]. In the first case, molecular geometry was completely optimized either at the Hartree–Fock or DFT

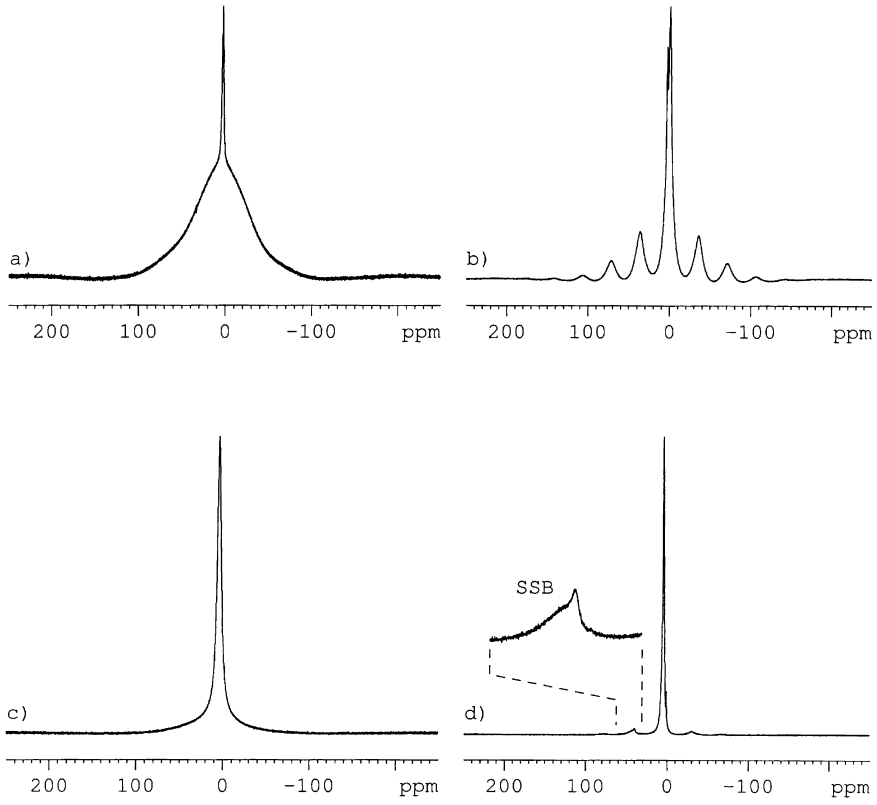

Fig. 3. (a) and (c) Static ^{1}H NMR spectra of products **TE-DM-1-1** and **TE**, respectively; (b) and (d) ^{1}H MAS NMR spectra of the same products, respectively. Static ^{1}H NMR spectra were measured by the solid-echo pulse sequence ($\pi/2_x-\tau_1-\pi/2_y-\tau_2-$aq). Delays τ_1 and τ_2 were 8 and 3 μs, respectively.

(B3LYP functional [36]) levels, the basis set being of the HF/6-31G* quality. For molecular mechanics calculation, a *cvff* force field was used.

3. Results and discussion

The considered siloxane materials are generally composed of four basic structure units (cf. Scheme 2) containing, in some cases, adsorbed water molecules.

As it is clear from a comparison of the ^{29}Si CP/MAS NMR spectra of the **TE**, **TE-DM-1-1** and **TE-DM-3-1** gels (Fig. 1a–c), modification of siloxane network by copolymerization of DMDEOS with TEOS causes both qualitative and quantitative changes. It follows from the "low-field" shift of signals of Q^n structural units in the modified gels that monomer units are rather uniformly placed in the bulk of the gel and do not form large separated domains containing one type of monomer units. The sufficiently uniform placement of monomer units is confirmed by narrow and symmetric lineshape of ^{29}Si NMR signals. A signal broadening and asymmetry would indicate huge heterogeneity and variability of local surroundings of monomer units. As it was confirmed by quantum-chemical calculations [26], the presence of the methyl groups decreases positive charge due to the positive inductive effect not only at the directly bonded ^{29}Si atom, but also at the neighboring atoms, and, consequently, makes a "low-field" shift of corresponding ^{29}Si NMR signals. This effect can be traced through several bonds. If there were very large domains of Q^n units in the product, such "low-field" shifts of their signals would not be possible or strongly diminished. These presumptions are proved by ^{29}Si CP/MAS NMR spectra of the **TE-DM-3-1** gel (Fig. 1c). Due to the initial composition of the reaction mixture, this product contains blocks of Q^n units and, consequently, the "low-field" shift of the ^{29}Si NMR signals of Q^n units is less apparent. From ^{29}Si NMR spectra of the reaction mixture of TEOS and DMDEOS presented in our previous work [26], it is clear that D^2 units are mainly built in cyclic copolymers and, in addition, do not form end groups. Chemical shifts of silicon of D^2 units have values from −19 to −15 ppm, which is the region of resonance of cyclic tetramers produced by copolymerization of both types of monomers.

As it follows from ^{1}H MAS NMR spectra (Figs. 1d–f and 2a and b), the nature and behavior of ≡Si–OH groups and adsorbed water molecules are dramatically changed by incorporation of D^2 units into the siloxane network. From the signal assignment [10,11,37], it is clear that **TE** gel contains mainly: (i) water and the silanols hydrogen-bonded to water molecules, which take part in chemical exchange

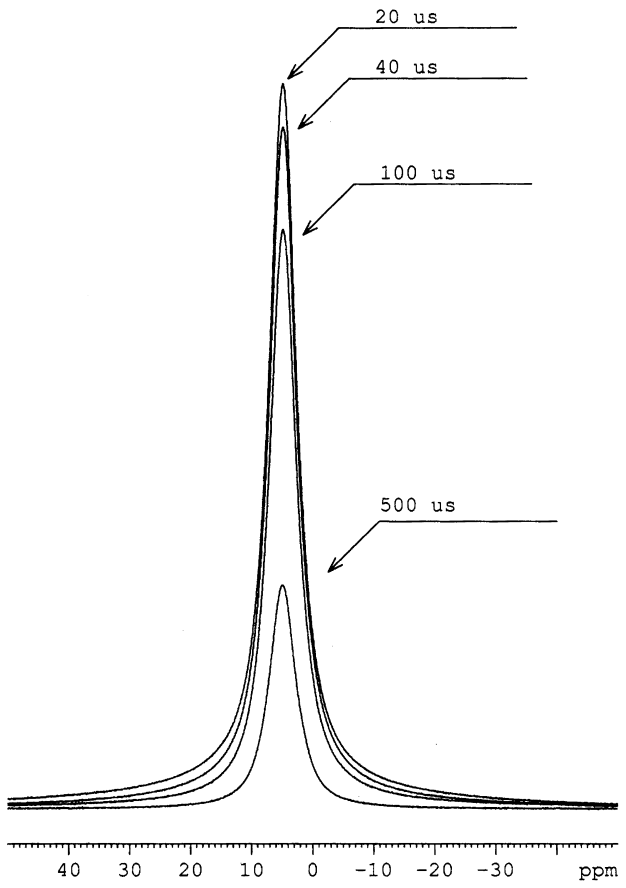

Fig. 4. ^{1}H MAS NMR spectra in absolute scale of product **TE** measured with the Hahn-echo pulse sequence with dipolar dephasing time increasing from 10 to 500 μs.

(4.79 ppm); (ii) water-inaccessible isolated silanols of Q^3 units (1.30 ppm); (iii) strongly coupled hydrogen-bonded silanols (broad signal at 6.45 ppm revealed after deconvolution); and (iv) the presence of such units was also confirmed from the shape of −1 (left) spinning side band as will be discussed later. By using a Hahn-echo pulse sequence ($\pi/2-\tau-\pi-\tau-$aq) with different dipolar dephasing times (for detailed experimental parameters, see Fig. 2); many other resonances appeared. Signals at ca. 3.80–2.90 ppm (a) correspond to weakly hydrogen-bonded silanols. A "high-field" signal at 1.06 ppm (b) can be attributed to the isolated single silanol, which is similar to the structure resonating at 1.30 ppm (c). The very weak "highest-field" signal resonating at ca. 0.0 ppm (d) was not assigned. In ^{1}H MAS NMR spectra of **TE-DM-1-1** (Figs. 1e and 2b), a relatively broad signal of methyl protons ≡Si–CH_3 (0.09 ppm) (e) and a narrow signal of silanols ≡Si–OH (3.42 ppm) (f) are dominant. A small amount of isolated silanols manifested by the signal at 1.34 ppm (g) (see Fig. 2b) is also present in the material. We can also assume the presence of strongly hydrogen-bonded silanols corresponding to a broad signal at ca. 6.5 ppm, which is, however, almost overlapped by a broad methyl resonance. With decreasing content of D^2 structure units in the material (**TE-DM-3-1**), chemical shift value of the signal of silanols shifts to the value of 3.96 ppm (Fig. 1f). This indicates the change in the nature of silanol groups and the presence of water molecules. Strongly hydrogen-bonded silanols are now clearly indicated by a broad signal at 6.43 ppm. The high degree of deshielding of this signal is due to very strong hydrogen-bonding interactions [37].

The content of water in modified materials was determined by comparing static ^{1}H NMR and single-pulse ^{29}Si MAS NMR spectra of both gels (**TE-DM-1-1**, **TE-DM-3-1**). The ratio of amounts of methyl and hydroxyl protons determined by deconvolution (i.e. computer separation of broad-Gaussian and narrow-Lorentzian components) of static ^{1}H NMR spectra (Fig. 3a) and ^{29}Si MAS NMR spectra is the same in both cases (12:1). From this it is clear that no water is adsorbed in the **TE-DM-1-1** gel. (The single pulse ^{29}Si MAS NMR spectrum is not shown here, because it is almost the same as ^{29}Si CP/MAS NMR one. The ratio of methyl and hydroxyl protons was determined from the integrated intensity of signals of D^2 and Q^2 and Q^3 units.) On the contrary, there is nearly one molecule of water per Si–OH group in the **TE-DM-3-1** gel because the ratios of methyl and hydroxyl protons determined by deconvolution of the ^{29}Si MAS NMR and ^{1}H NMR spectra have the values of 4.4:1 and 1.5:1, respectively.

3.1. $^{1}H-^{1}H$ dipolar interactions—proton dynamics

Analysis of the lineshapes of the ^{1}H NMR spectra measured under different experimental conditions and relaxation measurements were employed to evaluate molecular dynamics of protons. It is seen in Fig. 3a and b that a broad signal with a Gaussian lineshape of methyl protons in the static ^{1}H NMR spectra of **TE-DM-1-1** is substantially narrowed under MAS. The linewidth (full width at half intensity—f.w.h.i.) decreases from 15 to 1.2 kHz at the MAS frequency of 7 kHz. This fact together with the presence of intensive spinning side bands indicates strong homonuclear dipolar interactions of methyl protons. The Lorentzian signal of silanol groups with linewidth 480 Hz is narrowed by MAS only insignificantly. The linewidth of the signal thus reflects a large portion of incoherent processes (e.g. T_2 relaxation) and weak static dipolar interactions. The static ^{1}H NMR spectrum of **TE** (Fig. 3c) contains signal with linewidth 1100 Hz. The slightly asymmetric super-Lorentzian lineshape of this signal is caused by the superposition of a series of signals with different linewidths and chemical shifts, as it is proved by ^{1}H NMR spectra measured with the Hahn-echo pulse sequence. The gradual narrowing of the signal with the increasing dipolar dephasing delay time at the Hahn-echo pulse sequence (see Fig. 4) confirms the presence of differently mobile protons differing in the transverse T_2 relaxation rate, which indicates wide distribution of hydrogen bonding strengths in the **TE** gel. Dipolar dephasing time is so called T_2 filter, which strength depends on the length of the delay. Signal of very

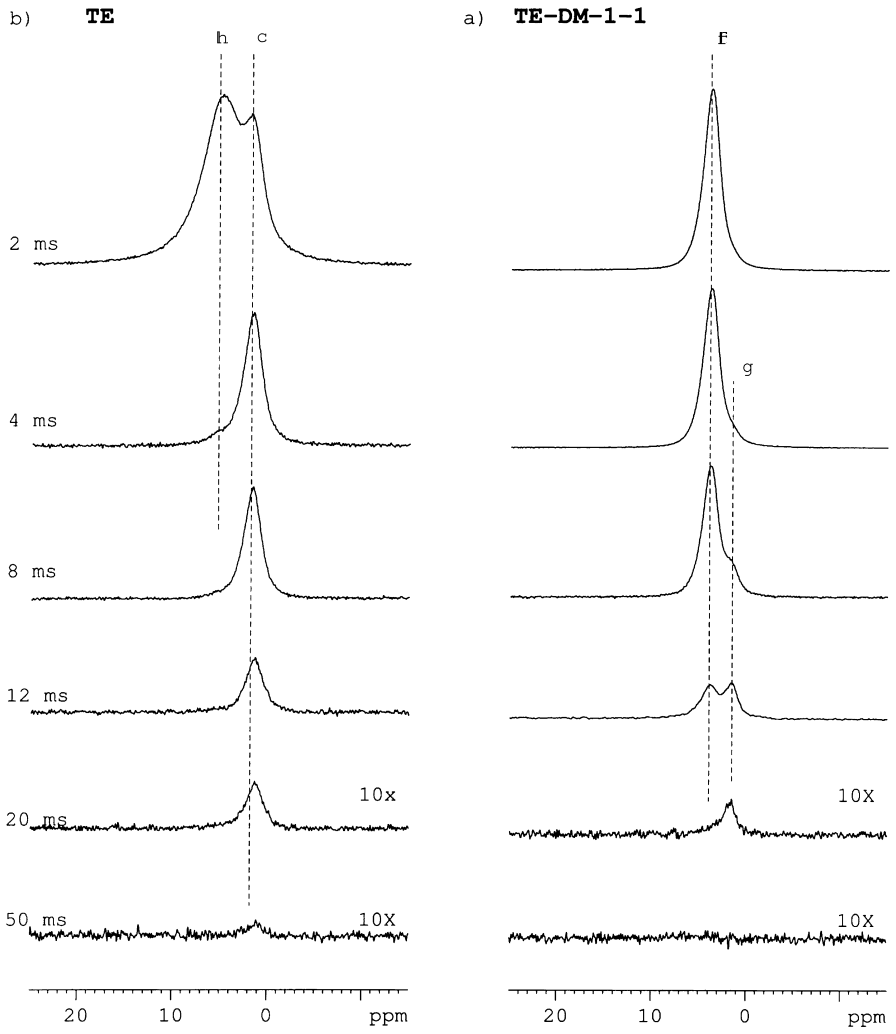

Fig. 5. Static ^{1}H NMR spectra of products **TE-DM-1-1** (a) and **TE** (b) measured with the Hahn-echo pulse sequence.

rigid molecules, which have very short T_2 relaxation time are substantially attenuated or canceled using relatively short dipolar dephasing period. Narrow signals of more mobile molecules are attenuated much later, during longer dipolar dephasing time. So the signals of rigid molecules, which are broad due to dipolar interaction disappear very fast and overall signal narrowing results. A MAS at 7 kHz narrows the signal to 417 Hz. This indicates line-broadening of the signal caused not only by incoherent processes (T_2 relaxation, chemical exchange, etc.) but also by coherent processes such as dipolar dephasing generated by static dipolar couplings, which can be, at least partially, refocused by MAS. However, arising spinning side bands (SSB) are very weak and asymmetric (Fig. 3d), which indicates weak static dipolar interactions between water and silanol protons. The asymmetry arises because of two components, one of high and one of low mobility. From the asymmetry of SSB, which is much larger compared with central band, it follows that protons of water molecules and large portion of silanols (at ca. 4.8 ppm) are relatively mobile (due to the weak dipolar interactions, MAS produces only weak SSB). Immobile protons of strongly hydrogen-bonded silanols (at ca. 6.5 ppm) have relatively more intensive spinning side bands under MAS due to their strong dipolar coupling. As both SSB signals of mobile and immobile protons are very closed and overlap, then due to different relative intensity of these signals the lager asymmetry of SSB compared with central signal results. (As MAS does not change the second moment of a line, intensive SSB under MAS conditions correspond to originally strongly dipolar-broadened signal in static NMR spectrum.)

The dipolar dephasing rate is an important probe of the effective strength of dipolar interactions. The above-mentioned standard Hahn-echo pulse sequence without MAS monitors dipolar dephasing caused by both coherent and incoherent processes. Under MAS and by an application of the refocusing π pulse, the coherent time evolution of the spin system can be inverted or can produce an echo. (Note that the homogeneous part of homonuclear interactions of abundant spins—bilinear interactions in the spin system—cannot be refocused completely [19,37–39].) Thus in the case of high-speed MAS with rates higher than 15 kHz,

Table 2
T_1 (^{1}H) times of some structural units in **TE** a **TE-DM-1-1** gels at different temperatures and calculated activation energies of their motion

T (K)	T_1(^{1}H) (ms)		
	TE	**TE-DM-1-1**	
	4.79 ppm[a]	3.42 ppm[b]	0.09 ppm[c]
303	222	713	747
318	252	740	771
333	282	785	807
343	302	805	837
E_a (kJ mol^{-1})	6.7	3.2	2.5

[a] Water and silanols hydrogen-bonded to water molecules.
[b] Weakly hydrogen-bonded silanols.
[c] Methyl protons ≡Si–CH_3.

we observe dipolar dephasing caused predominantly by the incoherent processes (relaxation), because the coherent effects are more or less averaged out, in particular in siloxane materials where protons are relatively diluted compared to organic solids.

During static dipolar dephasing experiment a broad signal of strongly coupled methyl protons in **TE-DM-1-1** sample is completely dephased within 80 μs. In contrast, the signal of Si–OH groups (3.42 ppm; f) diminishes at the dipolar dephasing period 15 ms and the signal of isolated silanols (1.34 ppm; g), which was at short dipolar dephasing times partially overlapped by the second broader signal, disappears at dephasing time 30 ms. This indicates weak and very weak dipolar interactions, respectively (Fig. 5a). The signal of exchanging water molecules and silanols in the **TE** gel (h) is dephased substantially faster (within 5 ms); however, the signal of single silanols at 1.30 ppm (c) is dephased slowly compared with the former case and it survives 50 ms of dipolar dephasing (cf. Fig. 5b). Small high field shift of this signal corresponds with inhomogeneous broadening of the signal reflecting at least two proton species. Dipolar dephasing is generally slowed down at high-speed MAS; the same rate of the dipolar dephasing under MAS and static conditions indicates that mainly incoherent processes (T_2 relaxation, chemical exchange, ^{1}H–^{1}H flip–flops and/or molecular motions) produce the magnetization decay. Significantly, the increase in the dipolar dephasing time of the methyl proton signal indicates a large portion of static dipolar interactions averaged by MAS. Both in **TE** and **TE-DM-1-1**, the signals of weakly hydrogen-bonded silanols (at ca. 3.5 ppm) disappear during 30 ms of the dipolar dephasing time and the signals of isolated silanols (at ca. 1.3 ppm) are not dephased even at 100 ms (cf. Fig. 2). This indicates the influence of coherent processes on dipolar dephasing and, consequently, the presence of static dipolar interactions. However, these interactions are relatively weak, which means that silanol protons in the **TEDM-1-1** product are not strongly coupled to methyl protons by dipolar interaction. Weak dipolar couplings originate either in the motional averaging of the labile species or in the long distances from other spins because dipolar interactions depend on r^{-6} (r is the internuclear distance). As we can assume relatively fast free rotation of methyl groups, a short dipolar dephasing time of methyl protons does not follow from restricted mobility but from anisotropy of the motion. Such anisotropy motion cannot average out homonuclear dipolar interactions. A very long dipolar dephasing time (>100 ms) of the signal at 1.3 ppm, assigned to isolated silanol protons, is given by a long distance of the silanol protons located on the network surface. It is important that the dipolar dephasing time and also the lifetime (about 30 ms) of the signal of hydrogen-bonded silanols (at 3.5 ppm) are nearly the same in the **TE** and **TE-DM-1-1** gels. This indicates the presence of similar or the same structures in both materials. We suppose that these structures correspond to small particles or domains formed by TEOS units located on the surface as well as in the inner part of network. Different dipolar dephasing times and chemical shifts of protons in the **TE** and **TE-DM-1-1** gels at 4.79 and 3.45 ppm, respectively, correspond with different strengths of hydrogen bonding of water molecules and silanols as well as with different mobilities and with the acidity of protons [40]. As the increase in dephasing lifetime of water and silanols (signal at 4.79 ppm) in the **TE** sample under MAS is not significant, incoherent processes like chemical exchange and molecular motion predominantly cause the coherence decay.

Longitudinal relaxation times T_1(^{1}H) and activation energies (calculated according to the Arrhenius law, see Table 2) in the **TE-DM-1-1** gel prove a higher molecular mobility of methyl groups compared with the mobility of water molecules and silanol groups in this gel. The presence of water in the **TE** gel increases the amount and variety of fluctuating magnetic fields and thus increases the relaxation rate. In addition, hydrogen bonds between water and silanols build up energy barriers restricting the mobility. However, from the temperature dependence it is clear that correlation times describing dipolar fluctuations and, consequently, motions of the detected protons are shorter than 5×10^{-9} s. Almost the same relaxation times T_1(^{1}H) for signals of methyl and silanol protons in the **TE-DM-1-1** product indicate communication between the two spin sets by means of spin diffusion, which equilibrates the magnetization behavior during a very long time, in the range from tens milliseconds to seconds. Using the formula for the maximum diffusive path length

$$L = (6DT_i)^{1/2} \quad (1)$$

where D is the spin diffusion coefficient and T_i is T_1(^{1}H), then from measured T_1(^{1}H) values the **TE-DM-1-1** material is homogeneous on a scale of ca. 25 nm [41,42]. (For the diffusivity, a value $D_{\text{eff}} = 0.136$ nm^2 ms^{-1} was determined from the proton line width, see section "^{1}H spin diffusion and molecular modeling" below.) Similar trends were also

Table 3
$T_{1\rho}$ (^{1}H) times of some structural units in **TE** a **TE-DM-1-1** gels at different temperatures and calculated activation energies of their motion

T (K)	$T_{1\rho}$(^{1}H), ms		
	TE	**TE-DM-1-1**	
	4.79 ppm[a]	3.42 ppm[b]	0.09 ppm[c]
303	5.29	3.65	15.70
318	5.78	7.22	16.81
333	6.55	10.00	17.08
343	6.77	12.21	18.34
E_a (kJ mol^{-1})	5.4	26.4	3.4

[a] Water and silanols hydrogen-bonded to water molecules.
[b] Weakly hydrogen-bonded silanols.
[c] Methyl protons ≡Si–CH_3.

observed in the case of longitudinal relaxation times in rotating frame $T_{1\rho}$(^{1}H)((Table 3). The high activation energy of silanol protons in the **TE-DM-1-1** gel (3.42 ppm) and the lowest relaxation time at 303 K correspond with the restricted motion and hydrogen bonds of silanol protons with bridged oxygen. The differences between the $T_{1\rho}$(^{1}H) relaxation times of silanol and methyl groups prove that dipolar interactions between them are too weak to equilibrate the magnetization behavior by means of spin diffusion during short spin lock times. Therefore, heterogeneities in the siloxane network are of a nanometer order.

The possibility to measure ^{29}Si NMR spectra using cross-polarization (CP) demonstrates the presence of relatively strongly heteronuclear- and homonuclear-coupled protons in both materials; the mobility of such protons has to be sufficiently restricted not to completely average out the Hamiltonian of heteronuclear and homonuclear dipolar interactions. ^{1}H–^{1}H dipolar-dephasing experiment (cf. Scheme 1d) monitors the effective strength of homonuclear interaction affecting the ^{1}H spin-state of these protons. The ^{1}H coherence decay of the protons coupled by the dipolar interaction with the silicon atoms is transferred by CP into the ^{29}Si spin state. During the dipolar dephasing period, τ_1, changes in the ^{1}H spin system (^{1}H–^{1}H flip–flop, chemical exchange, and molecular motion when the rate of motion of the ^{1}H–^{1}H internuclear vector is in intermediate region) cause non-refocusable ^{1}H magnetization decay [21]. Chemical shift anisotropy (CSA) and coherent processes generated by inhomogeneous part of static ^{1}H–^{1}H dipolar interactions cause modulation of the magnetization decay—echoes. Isotropic part of the ^{1}H chemical shift is refocused at any length of the τ_1 period. Coherent dipolar dephasing generated by inhomogeneous part of static dipolar interactions is refocused if τ_1 is equal to nt_r, where n is an integer and t_r is the MAS rotation period, whereas the anisotropic part of the chemical shift is completely refocused if $\tau_1 = 2nt_r$ [21].

^{1}H coherence decays for signals of both materials are very different (cf. Fig. 6). The decays of all three structure units Q^n in the **TE** gel are much slower compared with corresponding coherence decays in **TE-DM-1-1**. The signals of the Q^n units in the **TE** gel survive 1 ms of the dipolar dephasing period (it remains 8% of their original signal intensity). In addition, the modulation of the magnetization decay by refocusing CSA and coherent dipolar dephasing is less apparent. Thus at the 5 kHz spinning speed, preferentially incoherent processes and/or homogeneous dipolar interactions are the main source of the magnetization decay. This relatively fast decay compared with the ^{1}H magnetization decay directly detected in the ^{1}H NMR spectra for hydrogen-bonded water molecules and silanols (4.79 ppm in ^{1}H MAS NMR) indicates, that not all hydrogen-bonded water molecules are sufficiently close to protons participating in CP to affect their ^{1}H spin state or to be directly involved in the energy reservoirs for CP. This finding is confirmed by a 2D WISE experiment that is in principle very similar to the above-mentioned experiment. Linewidths of the ^{1}H slices in the 2D spectra of all structure units (Q^2, Q^3 and Q^4) are nearly the same (ca. 1.8 kHz, cf. Fig. 7). As they are larger than the linewidth of the signal in the ^{1}H MAS NMR spectra (478 Hz at 5 kHz of MAS frequency), it is clear that not all water and silanol protons, but only those with restricted mobility participate in CP. The presence of such protons corresponds with the presence of ±1 SSB with linewidth of ca. 1.7 kHz. In general, it follows that there are at least two groups of motionally or laterally different proton spins in the material. One of them being too mobile or too distant from the ^{29}Si nuclei to participate in CP. Hydrogen bonding or other interactions in the second reservoir of protons (not only protons indicated by the 'lowest-field' broad resonance at ca. 6.5 ppm) are sufficiently strong so that the consequently restricted motion cannot effectively average out the Hamiltonian of heteronuclear and homonuclear dipolar interactions. All ^{1}H signals were slightly narrowed to about 0.5 kHz by the introduction of the spin diffusion period (20 ms) confirming close spatial position and communication of water molecules with siloxane matrix (cf. Fig. 7b).

In contrast, the ^{1}H coherence decay of signals of the **TE-DM-1-1** gel units is much faster and more modulated by refocusing of coherent processes. The intensities of the signals of all three structure units (D^2, Q^3 and Q^4) reach the first minimum at 100 μs of the dipolar dephasing period (cf. Fig. 6) corresponding with the magnetization decay of methyl protons. It follows that methyl protons affect the ^{1}H spin-state of cross-polarizing protons and/or may be the main source for CP. The 2D WISE experiment confirms these statements because the lineshapes of ^{1}H slices of all units are very similar (cf. Fig. 7c). Silanol protons do not take part in the CP process, which is given by their weak homonuclear dipolar coupling with other proton spins (additionally weakened by MAS) and by the fact that the resulting heteronuclear coupling of nearly isolated spin pairs are easily spun into sidebands.

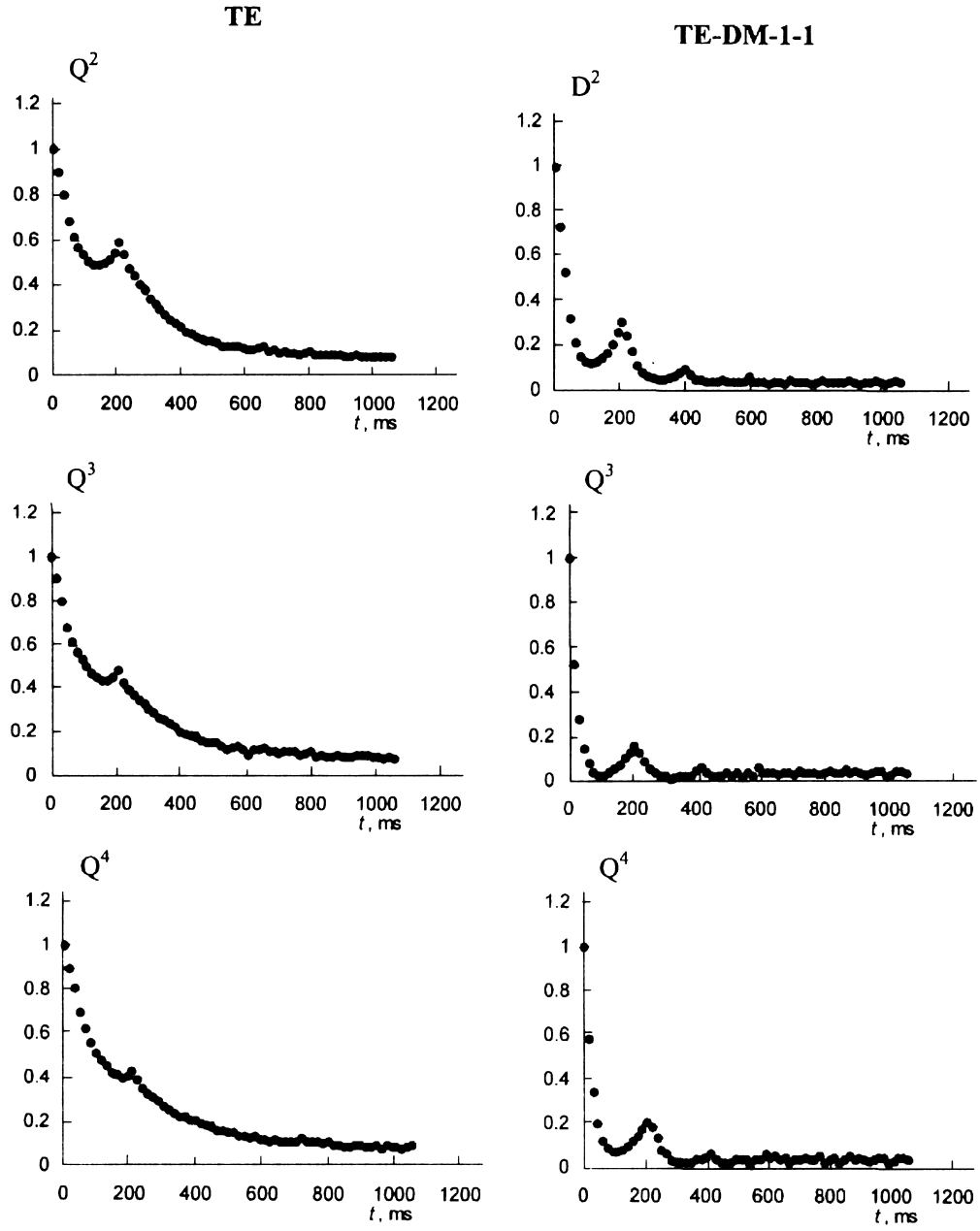

Fig. 6. ^{1}H coherence decays of D^2 and Q^n structure units signals of **TE-DM-1-1** and **TE** materials.

3.2. ^{1}H spin-diffusion and molecular modeling

To determine the size of heterogeneities and characterize the morphology of the system, a ^{1}H spin-diffusion experiment designed by Goldmann–Shen [30] was performed. This ^{1}H spin diffusion experiment is based on the presence of proton species differing in T_2 relaxation, which mutually communicate by means of dipolar couplings. In the static sample, the dipolar couplings are not averaged by MAS. The T_2 filter only selected the magnetization of silanol protons.

The evaluation of spin-diffusion curve was performed using to a strategy proposed by Schmidt-Rohr and Spiess [38] for a two-phase system with an interface and for variable dimensionality $\epsilon = 1$–3. As the general evaluation of spin diffusion process and derivation of all equations is well described in the literature [38,43] we present here only our basic considerations and predictions. The effective diffusivity, calculated according to the following equation:

$$\sqrt{D_{\text{eff}}} = \frac{2r\sqrt{D_{\text{OH}}D_{\text{Me}}}}{\sqrt{D_{\text{OH}}} + r\sqrt{D_{\text{Me}}}} \tag{2}$$

was used to simulate spin-diffusion process. The proton spin density ratio is defined as $r = \rho_{\text{Me}}/\rho_{\text{OH}}$. Diffusivity for silanol protons, which are located in TEOS particles, was

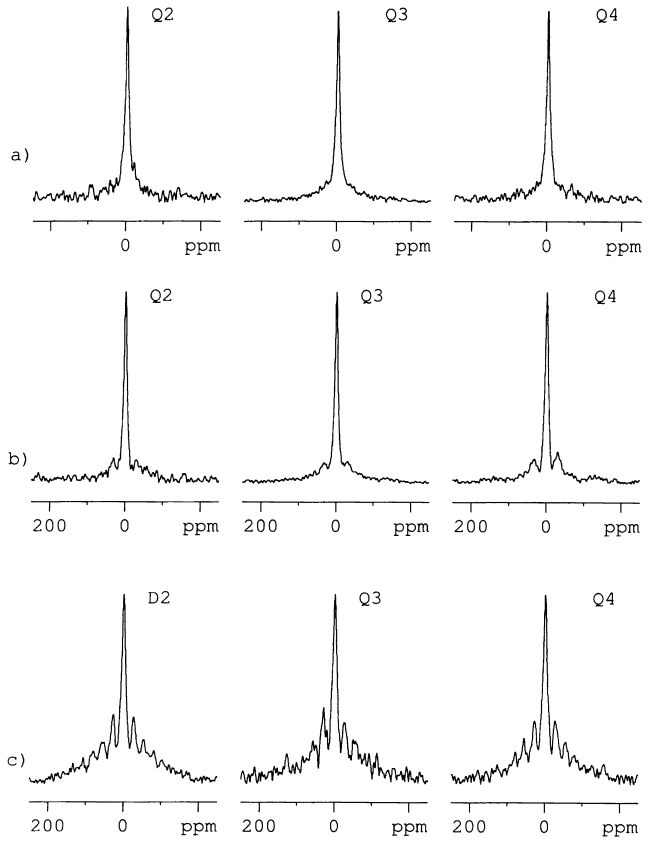

Fig. 7. (a) ^{1}H slices of 2D WISE spectra of Q^n structure units of **TE**; (b) ^{1}H slices of 2D WISE spectra with a spin diffusion period (20 ms) of the same structure units; (c) ^{1}H slices of 2D WISE spectra of D^2 and Q^n structure units of **TE-DM-1-1**.

calculated according to the following equation [43]:

$$D_{OH} = \frac{1}{6}\langle r^2\rangle[\alpha\Delta\nu_{1/2}]^{1/2} \quad (3)$$

where $\langle r^2\rangle$ is the mean-square distance between the nearest spins; α is cut-off parameter and $\Delta\nu_{1/2}$ is f.w.h.i. for the Lorentzian lineshape. Diffusion coefficient of methyl protons of copolymer phase was calculated from the equation, which is valid for Gaussian lineshape [43]:

$$D_{Me} = \frac{1}{12}\sqrt{\frac{\pi}{2\ln 2}}\langle r^2\rangle\Delta\nu_{1/2} \quad (4)$$

A rather gross simplification had to be made to evaluate $\langle r^2\rangle$ and spin density in the hybrid siloxane network. The two-component phase-separated system consisting of particles of DMDEOS monomer units on the one hand and of TEOS units on the other was chosen as the first model. All silanol protons are located in a part of TEOS monomer units because they are only slightly coupled by dipolar interaction to other (methyl) protons. (Dipolar broadening is relatively weak.) To determine the distances of silanol protons (only the nearest-neighbor proton–proton distances up to 0.5 nm were taken into account), a dimer of the earlier proposed [9,19] polycyclic basic structure unit containing nine silicon atoms was considered as a model compound (monomeric structure unit is shown in Fig. 9c). Owing to a high proportion of cyclization during polycondenzation of DMDEOS, cyclic tetramer (cyclooctamethyltetrasiloxane) was proposed as the simplest limit model for evaluating the proton–proton distance of methyl protons. The geometry of these units was optimized using molecular mechanics calculations. Calculated values, which are in a good agreement with interatomic distance in a cristobalite model [21] (for TEOS units), are listed in Table 4.

To extract domain sizes of both phases (TEOS phase—d_{OH} and copolymer phase—d_{Me}) as well as of the interface (d_i) from the spin diffusion experiment, the ratio of equilibrium NMR signal intensities $E = I_{OH}(eq)/I_{Me}(eq)$ and the ratio of spin densities r have to be determined [31,38,43]. They are related to the volume fraction of the dispersed phase by the expression

$$\Phi_{OH} = \frac{rE}{1+rE} = \left(\frac{d_{OH}+d_i}{d_{OH}+d_{Me}+2d_i}\right)^{\epsilon} \quad (5)$$

The value $E = 1/12$ obtained from the static ^{1}H NMR spectrum is inconsistent with the assumption that the system is formed only by two phases containing TEOS and DMDEOS monomer units, respectively. On the contrary, the calculated data indicate that ca. 50% of TEOS monomer units are directly built into the other phase, where DMDEOS units predominate. It is in accord with our findings [26] about the course of the early stages of copolymerization of TEOS and DMDEOS considering ca. 80% of DMDEOS units being built into the copolymers and 20% forming homopolymers after a five-day reaction. At the same time, 9% of TEOS units are not yet condensed, 54% form dimers and a small amount of short oligomers due to self-condensation, and 37% of TEOS units are included in the copolymers [26]. It follows that also the parameter r (ratio of spin densities) has to be corrected: the value $r = 2.05$ following from the aforementioned two component model consisting only of short oligomers was recalculated to $r = 2.46$. The higher value of r indicates a lower spin density of

Table 4
Calculated proton-proton mean distance $\langle r\rangle$; mean square distance $\langle r^2\rangle$; diffusion coefficients D_{OH} and D_{Me}; effective diffusion coefficient (D_{eff}= 0.136) D_{eff}; spin concentrations c_{OH} and c_{Me}; proton fraction Φ; density ρ_{OH} and ρ_{Me} and spin density $\rho(s)_{OH}$ and $\rho(s)_{Me}$

	$\langle r\rangle$ (nm)	$\langle r^2\rangle$ (nm^2)	D (nm^2 ms^{-1})	c	Φ	ρ (g cm^{-3})	$\rho(s)$ (g cm^{-3})
Silanol protons (OH)	0.37	0.162	0.013	0.077	0.016	1.96	0.038
Methyl protons (Me)	0.27	0.078	0.146	0.923	0.081	0.97	0.078

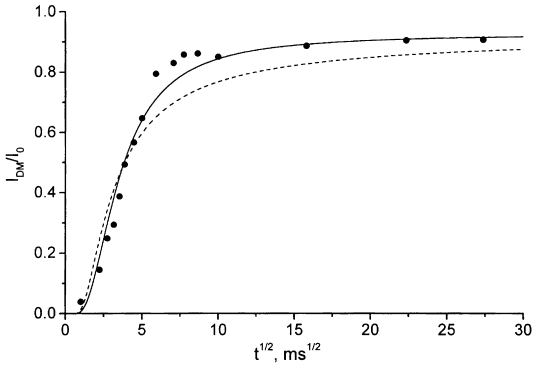

Fig. 8. Time dependence of NMR spin diffusion observables for the copolymer phase (filled circles). The continuous lines are calculated spin diffusion dependencies (dashed line for dimensionality $\epsilon = 1$, solid line for dimensionality $\epsilon = 2$). NMR spin diffusion observables for copolymer phase are the integrated intensities of broad component of static ^{1}H NMR spectra corresponding with methyls.

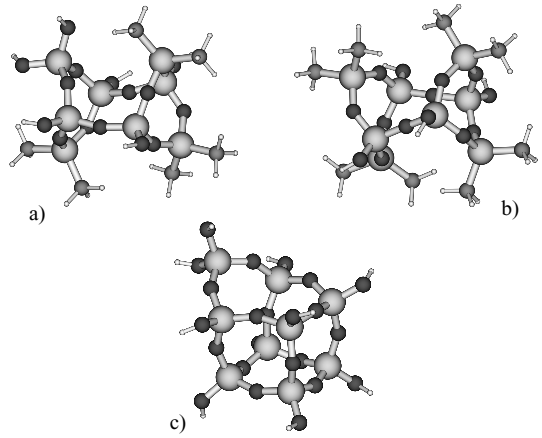

Fig. 9. Ab initio optimized geometry of the basic structure units calculated with the HF/6-31G* basis set.

homopolymer phase following from a higher condensation degree (decreased content of silanol protons) in contrast to the dimer model of polycyclic units. It should be noted that parameter r strongly affects calculated dimensions of individual phases as follows from Eq. (5). We suppose that the interfacial region is equally divided between the two main components.

It can be seen in Fig. 8 that the calculated diffusion curves of systems with 2D morphology well describe the experimental data for intermediate and long times. From a comparison of the experimental and calculated data (cf. Fig. 8 and Table 5), it is clear, that the material is nano-heterogeneous with the domain size of the TEOS homopolymer phase ca. 1.3 nm. The dimension of copolymer domains containing methyl groups is 2.1 nm. The presence of an interface between the copolymer and homopolymer phases results in the deviation of spin diffusion curves from linearity for small $t_m^{1/2}$ values. To determine the size of the interface, a spatially dependent spin diffusion coefficient was assumed varying linearly between the values D_{Me} and D_{OH}. The interface region is very small having the thickness ca. 0.5 nm. The so-called long period is then 4.4 nm.

All the above mentioned findings allow us to propose molecular structure of the hybrid siloxane network formed by copolymerization of TEOS and DMDEOS. The "low-field" shift of ^{29}Si NMR signals, different $T_{1\rho}(^1H)$ relaxation times, dipolar dephasing experiments, etc., indicate a nano-heterogeneous system, which is formed by relatively uniform structure units in both phases. The spin diffusion experiment confirmed this assumption, the calculated size of TEOS homopolymer domains is about 1.3 nm and the particle size in the copolymer phase is larger, ca. 2.1 nm. As was shown in our previous work [26], in the early stages of copolymerization, a diverse mixture of short homopolymer and copolymer chains forms with the number-average degree of polymerization ca. $\overline{P}_n = 4$–5. As cyclization is a significant process in polycondensation of alkoxysilanes and its importance increases with increasing reaction time, cyclic products form small building units of the arising gel. TEOS homopolymer particles are with high probability polycyclic units having 9–10 silicon atoms. The formation of such particles in polycondensation of TEOS is well discussed in the literature [9,19,44]. Chemical shifts of D^2 units in the ^{29}Si CP/MAS NMR spectra also reflect formation of polycyclic copolymers of DMDEOS and TEOS monomer units. The presence of single cyclic tetramers formed during polycondensation was confirmed by comparing calculated and experimentally determined ^{29}Si NMR chemical shifts [26]. In the present work, the geometry and ^{29}Si principal values of chemical shift tensors and isotropic chemical shifts of some of possible polycyclic condensed copolymers and homopolymers were optimized and calculated using ab initio calculations (cf. Fig. 9a and b). The obtained calculated and experimental data (only for the D^2 structure unit in the **TE-DM-1-1** material, determined from static ^{29}Si CP NMR spectra) are listed in Table 6. The experimental principal value of the ^{29}Si chemical shift tensor was determined from the best fit of static powder-pattern spectra and corrected for inhomogeneously broadened lineshape of central signal using Bruker program package WinFit. For comparison, the calculated principal value of the ^{29}Si chemical shift tensor of the inner silicon atom of linear trimer $(HO)(EtO)_2Si–O–Si(CH_3)_2–O–Si(EtO)_2(OH)$ are presented. All calculated data are relatively close to the experimentally determined

Table 5
Calculated domain size for different dimensionalities $\epsilon = 1$ and 2

	$\epsilon = 1$	$\epsilon = 2$
d_{OH} (nm)	0.3	1.3
d_{Me} (nm)	3.8	2.1
d_i (nm)	0.6	0.5
$d = d_{OH} + d_{Me} + d_i$	5.3	4.4

Table 6
Experimental and calculated (HF/6-31G*) ^{29}Si principal values of chemical shift tensors. Isotropic shift values were calculated as the trace, i.e. $\delta_{iso} = 1/3(\delta_{11} + \delta_{22} + \delta_{33})$. Asymmetry parameter η was calculated as: $\eta = (\delta_{22} - \delta_{11})/\delta_{33}$

Structure	Atom No.	δ_{11} calc. (ppm)	δ_{22} calc. (ppm)	δ_{33} calc. (ppm)	δ_{iso} calc. (ppm)	η
Linear		11.0	−0.2	−63.1	−17.4 [−19.9 to −20.9][c]	0.18
I[a]	1	15.9	13.6	−54.3	−8.3	0.04
	2	16.3	13.7	−50.5	−6.9	0.05
	3	14.8	13.1	−53.3	−8.5	0.03
II[b]	1–4	14.6	13.7	−51.0	−7.5	0.02
Experimental data		δ_{11} expt (ppm)	δ_{22} expt (ppm)	δ_{33} expt (ppm)	δ_{iso} expt [δ_{iso} MAS] (ppm)	
TE-DM-1-1	D^2	2	−2	−52	−17.3 [−17.3]	0.07

[a] See Fig. 9a.
[b] See Fig. 9b.
[c] Experimentally determined chemical shift from high resolution ^{29}Si NMR spectra [26].

values confirming copolymerization. Although at this level of theory the calculated data of chemical shift principal values do not enable an unambiguous assignment of the specific structure units, parameters of asymmetry indicate formation of cyclic structure. As the changes caused by cyclization and formation of polycyclic units are relatively small to be reflected in the calculated values of the chemical shift tensor at a given level of theory, formation of a small portion of linear structures cannot be quite excluded.

From all the aforementioned data it follows that the siloxane material is formed by copolymer and homopolymer particles. However, the discussed cyclic copolymers alone can hardly form a strong infinite network because their effective functionality is relatively low ($f = 2$–3); in addition, it is well known that the formation of alkyl(alkoxy)silane network with functionality $f = 3$ is complicated due to high cyclization during polycondensation [19]. Although the morphology of the siloxane materials is not known, we suggest so-called "bicontinuous, random morphology" [45]. This means that there are two infinite and continuous networks, which are interlaced as well as chemically bonded together. The relatively thin network of TEOS homopolymers provides strength and consistency and the larger but weaker copolymer network fills the former one. Our suggestion corresponds with the determined dimensionality which is between $\epsilon = 2$ and $\epsilon = 1$. Introducing the dimensionality as the number of orthogonal directions relevant for the spin diffusion process, one can imagine a 2D spin diffusion process in siloxane network branches and a 1D process at network junctions.

4. Conclusion

All the above mentioned results allow us to conclude that modification of siloxane network by copolymerization of DMDEOS and TEOS causes a series of structure changes.

In the modified siloxane network, the amount of water is significantly reduced down to its absence. In a non-modified siloxane material, a part of water and silanol protons is very mobile and participates in the chemical exchange. Although they do not directly participate in cross-polarization, they are still sufficiently close to the other part, immobile, cross-polarizing protons, to affect their spin system. In the modified siloxane network, where no water is tensors and the isotropic chemical shift support our predictions that copolymers with polycyclic structure units are predominantly formed. As such particles alone can only hardly form infinite network, the TEOS homopolymer layer provides its cohesion (consistency).

Acknowledgements

The authors thank the Grant Agency of the Czech Republic for its financial support (grant 203/98/P290 and 203/97/0539).

References

[1] Brunet F, Cabane B. J Non-Cryst Solids 1993;163:211.
[2] Brunet F, Cabane B, Dubois M, Perly B. J Phys Chem 1991;95:945.
[3] Lux P, Brunet F, Desvaux H, Virlet J. Magn Reson Chem 1993;31:623.
[4] Pouxviel JC, Boilot JP, Beloeil JC, Lallemand JY. J Non-Cryst Solids 1987;89:345.
[5] Sanchez J, McCormic A. J Phys Chem 1992;96:8973.
[6] Fyfe CA, Aroca PP. Chem Mater 1995;7:1800.
[7] Sanchez J, McCormic A. J Non-Cryst Solids 1994;167:289.
[8] Liu Juwhan, Kim Sun Dun. J Polym Sci 1994;34:131.
[9] Kudo T, Gordon MS. J Am Chem Soc 1998;120:11 432.
[10] Vega AJ, Scherer GW. J Non-Cryst Solids 1989;111:153.
[11] Bronnimann CE, Zeigler RC, Maciel GE. J Am Chem Soc 1988;110:2023.
[12] Beshah K, Mark JE, Ackerman JL. J Polym Sci B, Polym Phys 1986;24:1207.
[13] Maciel GE, Sindorf DW. J Am Chem Soc 1980;102:7606.
[14] Sindorf DW, Maciel GE. J Am Chem Soc 1981;103:4263.
[15] Sindorf DW, Maciel GE. J Am Chem Soc 1983;105:1487.
[16] Sindorf DW, Maciel GE. J Phys Chem 1982;86:5208.
[17] Sindorf DW, Maciel GE. J Am Chem Soc 1983;105:3767.
[18] Sindorf DW, Maciel GE. J Phys Chem 1982;87:5516.
[19] Devreux F, Boilot JP, Chaput F, Lecomte A. Phys Rev A 1990;41:6901.

[20] Malier L, Devreux F, Chaput F, Boilot JP, Axelos MAV. J Non-Cryst Solids 1992;147:686.
[21] Chuang I-S, Kinney DR, Bronnimann CE, Zeigler RC, Maciel GE. J Phys Chem 1992;96:5516.
[22] Yen Wei, Dachuan Yang, Bakthavatchalam R. Mater Lett 1992;13:261.
[23] Babonneau F. New J Chem 1994;18:1065.
[24] Deng Q, Moore RB, Mauritz KA. J Appl Polym Sci 1998;68:747.
[25] Iwamoto T, Morita K, Mackenzie JD. J Non-Cryst Solids 1993;159:65.
[26] Brus J, Dybal J. Polymer 1999;40:6933.
[27] Pines A, Gibby MG, Waugh JS. J Chem Phys 1973;70:3300.
[28] Schmidt-Rohr K, Clauss J, Spiess HW. Macromolecules 1992;25:3273.
[29] Zumbulyadis N. Phys Rev B 1986;33:6495.
[30] Goldmann M, Shen L. Phys Rev 1966;144:321.
[31] Clauss J, Schmidt-Rohr K, Spiess HW. Acta Polym 1993;44:1.
[32] Chin YH, Kaplan S. Magn Reson Chem 1994;53:32.
[33] Alemany LB, Grant DM, Alger TD, Pugmire RJ. J Am Chem Soc 1983;105:6697.
[34] Frisch MJ, Trucks GW, Schlegel HB, Gill PMW, Johnson BG, Robb MA, Cheeseman JR, Keith T, Petersson GA, Montgomery JA, Raghavachari K, Al-Laham MA, Zakrzewski VG, Ortiz JV, Foresman JB, Cioslowski J, Stefanov BB, Nanayakkara A, Challacombe M, Peng CY, Ayala PY, Chen W, Wong MW, Andres JL, Replogle ES, Gomperts R, Martin RL, Fox DJ, Binkley JS, Defrees DJ, Baker J, Stewart JP, Head-Gordon M, Gonzalez C, Pople JA. GAUSSIAN 94, Revision E.2, Gaussian, Inc., Pittsburgh PA, 1995.
[35] INSIGHT II Version 95.0 Molecular Modeling System, BIOSYM/MSI 1995.
[36] Becke AD. J Chem Phys 1993;98:1372.
[37] Jean Baptiste d'Espinose de la Caillerie, Aimeur MR, Kortobi YE, Legrand AP. Coll Interf Sci 1997;194:434.
[38] Schmidt-Rohr K, Spiess HW. Multidimensional solid-state NMR and polymers, New York: Academic Press, 1994 p. 126–32.
[39] Maricq MM, Waugh JS. J Chem Phys 1979;70:3300.
[40] Pfeifer H. J Chem Soc, Faraday Trans 1 1988;84:3777.
[41] Schmidt P, Straka J, Dybal J, Schneider B, Doskočilová D, Puffr R. Polymer 1995;36:4011.
[42] Matsumoto A, Egama Y, Matsumoto T, Horii F. Polym Adv Technol 1997;8:250.
[43] Demco DE, Johanson A, Tegenfeldt J. Solid State Nucl Magn Reson 1995;4:13.
[44] Ng LV, Thompson P, Sanchez J, Macosko CW, McCormic A. Macromolecules 1995;28:6471.
[45] Ryan AJ, Stanford JL, Sill RH. Plast Rubber Process Appl 1990;13:99.